Chapter 4

Polarization and Thermally Stimulated Processes in Lead-Free Ferroelectric Ceramics

Aimé Peláiz-Barranco, Yuslín González Abreu, José de los Santos Guerra, Jinfei Wang, Tongqing Yang and Pierre Saint-Grégoire

Additional information is available at the end of the chapter

http://dx.doi.org/10.5772/60433

Abstract

Over the last 20 years there has been an enormous effort in developing lead-free ferroelectric ceramics in order to obtain good dielectric, ferroelectric, piezoelectric and pyroelectric properties than those the conventional ferroelectric ceramics based on lead, such as lead zirconate titanate. An important group of lead free ferroelectric materials belong to the Aurivillius family, compounds which are layered bismuth $[Bi_2O_2]^{2+}[A_{n-1}B_nO_{3n+1}]^{2-}$. $SrBi_2Nb_2O_9$ is a member of this family where the ferroelectric properties can be affected by the crystallographic orientation due to their anisotropic crystal structure. The divalent Sr cation located between the corner-sharing octahedra can be totally or partially replaced by other cations, most commonly barium. The chapter presents the analysis of the thermally stimulated current in $Sr_{1-x}Ba_xBi_2Nb_2O_9$ ferroelectric ceramic system with x = 0, 15, 30, 50, 70, 85, 100 at%. A numerical method is used to separate the real pyroelectric current from the other thermally stimulated processes. The remanent polarization is evaluated considering the hysteresis ferroelectric loops; the pyroelectric coefficient and the merit figure are evaluated too. $Sr_{0.70}Ba_{0.30}Bi_2Nb_2O_9$ shows better ferroelectric and pyroelectric properties.

Keywords: Ferroelectrics, Aurivillius, Ceramics, Polarization, Pyroelectricity

1. Introduction

It is known that lead-based ferroelectric systems exhibit very good properties for different kinds of applications [1-6] and also that high-level ferroelectric and piezoelectric activities have remained confined to these materials. The only drawback in the technology as a whole has been the environmentalist's nightmare of its dependence on a high lead-containing family of materials [7]. Therefore, over the last 20 years there has been an enormous effort made in developing lead-free ferroelectric systems in order to obtain better dielectric, ferroelectric, piezoelectric and pyroelectric properties than those of conventional ferroelectric ceramics based on lead, such as lead zirconate titanate (PZT) [8-10].

An important group of lead-free ferroelectric materials belong to the Aurivillius family $\{[Bi_2O_2]^{2+}[A_{m-1}B_mO_{3m+1}]^{2-}\}$, which was discovered by Bent Aurivillius in 1949 [11]. These compounds have a complex structure, which is composed of perovskite blocks ($[A_{m-1}B_mO_{3m+1}]^{2-}$) interleaved between bismuth and oxygen layers ($[Bi_2O_2]^{2+}$), where *m* is the number of perovskite blocks in the structure. The *A* sites of the structure are typically occupied by elements such as Sr^{2+}, Ba^{2+}, Ca^{2+} and Bi^{3+}, with low valence; the *B* sites are typically occupied by elements with high valence such as Ti^{4+}, Nb^{5+} and W^{6+} [12-16]. These materials have received great attention due to their large remanent polarization, low real dielectric permittivity at room temperature, lead-free nature, relatively low processing temperatures, high Curie temperatures, high electromechanical anisotropy and coercive fields, and excellent piezoelectric properties [8-9], which have suggested them as good candidates for high-temperature piezoelectric applications and memory storage. The bismuth layers $[Bi_2O_2]^{2+}$ constrain the size of perovskite blocks establishing a limit for the incorporation of elements into them and providing the mixing of different elements between *A* sites and bismuth sites in the layered structure [17]. The ferroelectricity depends strongly on the crystallographic orientation of these materials, which is the subject of continuing researches. The main contribution to its spontaneous polarization comes from the displacement of the *A* cation in the perovskite block, which is quite different for the perovskite structure. It is well known that these have the majority polarization vector along the a-axis in a unit cell and that the oxygen vacancies prefer to stay in the Bi_2O_2 layers, where their effect upon the polarization is thought to be small, and not in the octahedral site that controls polarization [18].

Figure 1 shows the structure for some Aurivillius systems with m=1, m=2 and m=3, at the paraelectric phase, as examples. The structural studies on these materials have shown a relation between the number of perovskite blocks and the symmetry of the cell, i.e., the number of perovskite blocks is related to the crystallographic orientation and to the plane of polarization in these materials [12-16, 18-19]. The polarization vector has also shown a relation to the number of perovskite blocks [18]. For even-layered systems, it has been reported to be a restriction on the polarization to the *a-b* plane of the cell and an orthorhombic symmetry with $A2_1am$ space group [18]. For odd-layered systems, the polarization has shown a component in c and orthorhombic phase with *B2cb* space group [18]. Other results have shown a strong relation between the elements in *A* sites of the structure and the symmetry of the cell [13-14, 17].

http://dx.doi.org/10.5772/60433

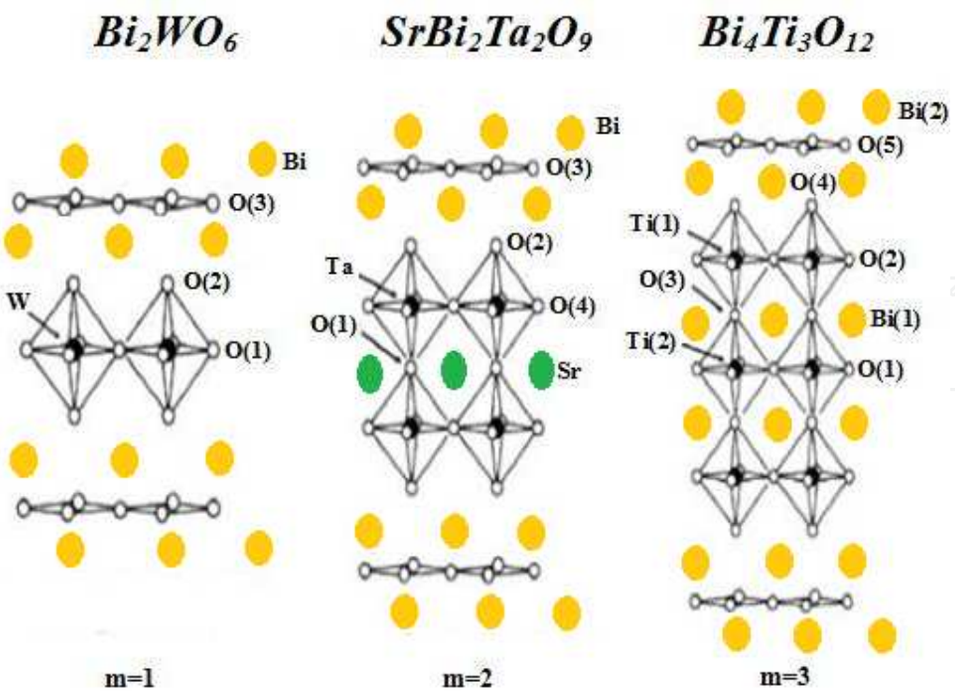

Figure 1. Structure of some Aurivillius materials with m=1, m=2 and m=3, at the paraelectric phase.

$SrBi_2Nb_2O_9$ (SBN) is a member of the Aurivillius family in which the ferroelectric properties can be affected by the crystallographic orientation due to their anisotropic crystal structure [13-14]. This system has received particular attention due to its large fatigue resistance, which has been associated with the migration of oxygen vacancies in the material [20]. The Sr^{2+}cation, which is located between the corner-sharing octahedral, can be totally or partially replaced by other cations, as barium is an important element for improving fatigue resistance [20]. The studies on the barium-modified $SrBi_2Nb_2O_9$ system have shown interesting results from the structural and dielectric point of view [13-14, 20-25]. Structural studies have shown an orthorhombic symmetry with $A2_1am$ space group for pure and doped SBN samples [22]. The mixing of different elements between *A* sites and bismuth sites, which occurs to equilibrate the lattice dimensions between the $(Bi_2O_2)^{2+}$ layers and the perovskite blocks, has been also analysed [22]. The oxygen vacancies, which are the results of Bi^{3+} for Ba^{2+}/Sr^{2+} substitution, could have an important influence in the properties of these compositions [22].

For the $Sr_{1-x}Ba_xBi_2Nb_2O_9$ system (x= 0, 15, 30, 50, 70, 85, 100 at%), the barium concentration dependence of T_m, as well as the temperature of the corresponding maximum for the real part of the dielectric permittivity, has suggested a cation site mixing among atomic positions, which has been supported by structural analysis [22]. For compositions with $x \leq 30$ at%, T_m increased with the barium concentration; for $x \geq 50$ at%, a decrease of T_m and a widening of the curves was observed with the increase of the barium concentration. The structural studies have shown the mixing of Sr^{2+}, Ba^{2+} and Bi^{2+} into *A* sites and the bismuth sites of the structure [22]. For lower barium concentrations ($x \leq 30$ at%), the presence of bismuth into *A* sites and the increasing of the strontium concentration into this site, has been discussed as the principal reason for the

increase of the T_m value. The higher barium concentration into A sites was obtained for the compositions with x ≥ 50 at% [22], supporting the decreasing of T_m [22].

On the other hand, a change from normal ferroelectric-paraelectric phase transition to relaxor behaviour has been observed when the barium concentration is increased [22]. For the compositions showing relaxor behaviour, an increase of the frequency dispersion degree was also observed with the increase of barium concentration. The relaxor behaviour is typical of materials with a disorder distribution of different ions in equivalent sites of the structure, which is called compositional disorder. For the studied materials, the relaxor behaviour has been explained with reference to the positional disordering of cations at A sites of the structure, which delays the evolution of long-range polar ordering [23, 26].

1.1. Ferroelectric behaviour and pyroelectricity in ferroelectric materials

It is known that ferroelectric materials present a spontaneous polarization in the absence of an electrical field (E), for temperatures below the temperature of the phase transition from the ferroelectric to the paraelectric phase [1]. These materials have regions with uniform polarization, which are called ferroelectric domains. If an electrical field is applied to the material, the structure of domains changes due to the reorientation of the dipoles with E. In ferroelectrics with normal ferroelectric-paraelectric phase transitions, if the electrical field is strong enough the system can reach a saturated state, showing a high percentage of oriented domains in the E direction, which depends on the structure of the system. When the electrical field is removed, the system exhibits a remanent polarization (P_r), which corresponds to the configuration of the minimal energy. On the other hand, for relaxor ferroelectrics, typical slim loops suggest that most of the aligned dipole moments switch back to a randomly oriented state upon removal of the field.

Ferroelectric materials, good isolators by their nature, exhibit temperature-dependent polarization, i.e., when the sample is heated the polarization changes and an electrical current is produced (pyroelectric current) which disappears at a certain temperature [1]. For normal ferroelectrics, the pyroelectric current (i_p) achieves a maximum value when the temperature (T) increases, and then decreases until zero at the ferroelectric-paraelectric phase transition temperature. For relaxor ferroelectrics, the pyroelectric current is different from zero even at higher temperatures than T_m, as well as the temperature of the corresponding maximum for the real part of the dielectric permittivity [27].

However, the study of the pyroelectric behaviour and its corresponding physical parameters may be quite difficult in many ferroelectric systems because, apart from the localized dipolar species, free charges can also exist in the material. The decay of the electrical polarization could be due to dipolar reorientation, the motion of the real charges stored in the material and its ohmic conductivity. The first of these is induced by thermal excitation, which leads to decay of the resultant dipole polarization, and the second is related to the drift of the charges stored in the internal field of the system and their thermal diffusion. During the temperature rise, the dipoles tend to be disordered gradually owing to the increasing thermal motion, and the space charges trapped at different depths are gradually set free. Therefore the pyroelectric behaviour is usually overlapped by other thermally stimulated processes, and a detailed analysis of this

http://dx.doi.org/10.5772/60433

phenomenon is very important in order to separate the different components of the electrical current during the heating of the material (*i-T* dependences), to then make a real pyroelectric characterization of any system.

The thermally stimulated discharge current method is a typical technique for this analysis, which has been applied with very good results to ferroelectric materials [28-30]. By using this method, the pyroelectric current can be separated from other stimulated processes (including the electrical conductivity mechanisms), providing better knowledge of the material response in a wide temperature range.

Several analytical methods have been developed to analyse the thermally stimulated processes [30-33]. Among these can be mentioned the initial rise method, the peak shape method and the numerical method using Gaussians [30-33].

For the initial rise method, it is considered that measurements do not depend on the heating rate in the initial rise region [33]. Then, a slow heating rate can be used, reducing the problems related to the difference of temperature between the samples and the thermocouple or gradients of temperature in the sample. The peak shape methods [34] depend on the constant heating rate, but consider more experimental points concerning the initial rise method. However, these methods do not consider the overlapping of several peaks in the material response, as the Gaussian method does. This method considers the overlapping of several peaks in *i-T* dependences, which is very useful for a better understanding of the material response.

The Gaussian method was proposed by Faubert and Sánchez [32]. It consists of fitting the rightmost part (highest temperatures) of the curve with a single time relaxation theoretical curve (Gaussians), and then a new spectrum is obtained by subtracting the theoretical curve from the experimental one (Figure 2). The operation is repeated until the resulting spectrum is smaller than a fixed limit. The final test is carried out summing all the theoretical curves, which may offer the experimental spectrum.

From the so-called area method given by equation (1), where T_F is the final temperature and β is the constant heating rate, which is constant, the relaxation times (τ) can be calculated for each theoretical curve (single curves). On the other hand, it is known that the relaxation times usually show a temperature dependence which can be expressed by the Arrhenius law (equation 2, where k_B and τ_0 are constants). Then, the activation energy value (U) for each process can be obtained from the ln τ vs $1/T$ dependence.

$$\tau(T) = \frac{\int_T^{T_f} i(T)dT}{\beta.i(T)} \tag{1}$$

$$\tau(T) = \tau_0 e^{\frac{U}{k_B T}} \tag{2}$$

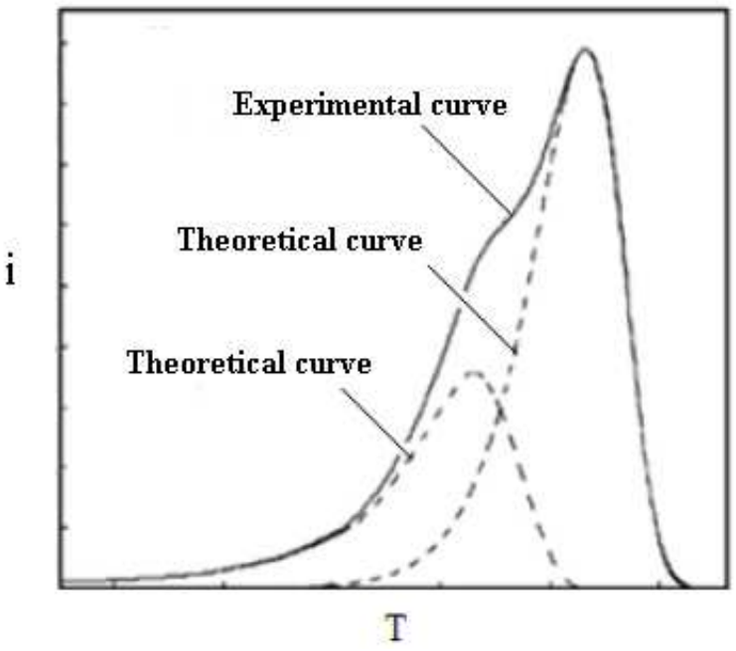

Figure 2. Theoretical decomposition of the *i*-*T* dependence using the Gaussian method.

The remanent polarization (P_r) can be obtained from the pyroelectric current $i_p(T)$ using equation 3, where A is the area of the samples. The integration is made from the operation temperature T (usually room temperature) until T_m (or a higher temperature in the case of relaxor ferroelectrics).

$$P_r = -\frac{1}{A\beta}\int_{T}^{T_m} i_p dT \tag{3}$$

Other parameters can be evaluated from the $i_p(T)$ dependence, such as the pyroelectric coefficient (p) and several merit figures. The pyroelectric coefficient is related to the variation of P_r (equation 4). The current response parameter (R_v) is one of the important merit figures which are associated with pyroelectric behaviour, and can be obtained using equation 5.

$$p = \frac{dP_r}{dT} \tag{4}$$

$$R_v = \frac{p}{\varepsilon'} \tag{5}$$

There are not many reports concerning the pyroelectric behaviour of ferroelectric systems from the Aurivillius family. Most of the studies have been carried out on pure and modified bismuth

http://dx.doi.org/10.5772/60433

titanate [35-36]. For niobium- and thallium-modified bismuth titanate, it has been reported that there is a pyroelectric coefficient of 12 μC/m²K at room temperature [36], which is better than that for pure bismuth titanate ceramics [35]. The *P-E* hysteresis loops have showed a remanent polarization of 3.49 μC/cm² at room temperature [36].

The chapter presents studies on ferroelectric properties and thermally stimulated processes which have been carried out on the $Sr_{1-x}Ba_xBi_2Nb_2O_9$ ferroelectric ceramic system with x = 0, 15, 30, 50, 70, 85 and 100 at%. The dependence of the polarization on the applied electric field is discussed at room temperature, for normal and relaxor ferroelectrics compositions. For the thermally stimulated current, the Gaussian method is used to separate the pyroelectric contribution from the other contributions to the total *i(T)* response in the studied samples. The remanent polarization is evaluated, at room temperature, considering the hysteresis ferroelectric loops and the pyroelectric current dependence $i_P(T)$. The pyroelectric coefficient and the current response merit figure are also evaluated.

2. Experimental Procedure

2.1. Sample preparation

$Sr_{1-x}Ba_xBi_2Nb_2O_9$ (x = 0, 15, 30, 50, 70, 85, 100 at%) ferroelectric ceramic samples were prepared by solid-state reaction method (Figure 3).

The powders of the starting materials SrO, BaO, Bi_2O_3 and Nb_2O_5 were mixed with a desired weight ratio. The mixture of oxides was milled with alcohol for two hours, dried and pressed by applying 100 MPa. The pressed samples were calcined in air atmosphere at 950 °C for two hours. After calcination the samples were milled again for one hour, dried and pressed by applying 200 MPa. The sintering process was made in a sealed alumina crucible at 1100 °C for one hour. Samples with density values higher than 90 % of the theoretical density values were obtained. Silver electrodes were deposited on the opposite faces of the disk-like samples by using a heat treatment at 590 °C. The samples were named SBN (x=0), SBBN-x (x=15-85 at%) and BBN (x=100 at%), respectively.

2.2. Ferroelectric measurements and thermally stimulated discharge current experiments

Polarization-electric field (*P–E*) loops were obtained at room temperature for 10 Hz by using a precision ferroelectric analyser (Premier II, Radiant Technologies Inc.), which is combined with a high-voltage power supply (TReK Model 663A). The highest applied electric field was 90 kV/cm for the studied samples.

The study of thermally stimulated depolarization currents was carried out in sequential thermal cycles as follows: (*i*) zero-field heating - heating from room temperature to 60 °C under zero electrical field; (*ii*) field cooling – cooling to room temperature while a polarizing electrical field is applied (E_P = 2 kV/mm); (*iii*) zero-field heating – heating from room temperature to temperatures higher than T_m under zero electrical field. The thermal discharge current was

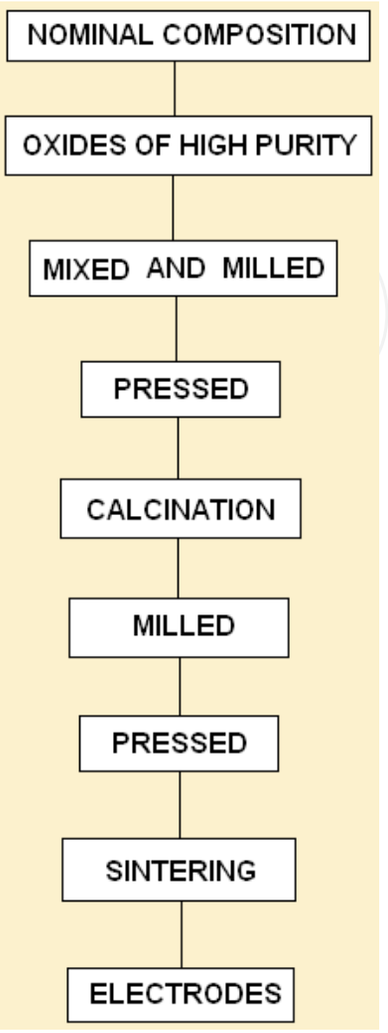

Figure 3. Solid-state reaction method for the sample preparation.

measured (during the third step) using a Keithley 6485 Electrometer, while keeping a temperature rate of about 5 K/min.

3. Results and discussion

3.1. Ferroelectric properties

The hysteresis loops at room temperature are shown in Figure 4 and Figure 5 for the studied samples. The compositions with $x \leq 30$ at% show polarization-electrical field (P–E) loops typical of normal ferroelectric materials. The compositions of SBN and SBBN-15 show wide loops at room temperature. This behaviour could be associated with high dielectric losses in these samples. The composition with 30 at% of barium shows the better response with a clear tendency to saturation with the applied electric field. The samples with $x \geq 50$ at% show thin hysteresis loops, which are typical of relaxor ferroelectric systems. These compositions have

http://dx.doi.org/10.5772/60433

shown relaxor behaviour in the corresponding dielectric analysis [22]; relaxor ferroelectrics do not show a tendency to saturation in the *P*–*E* dependence even in a very high electric field.

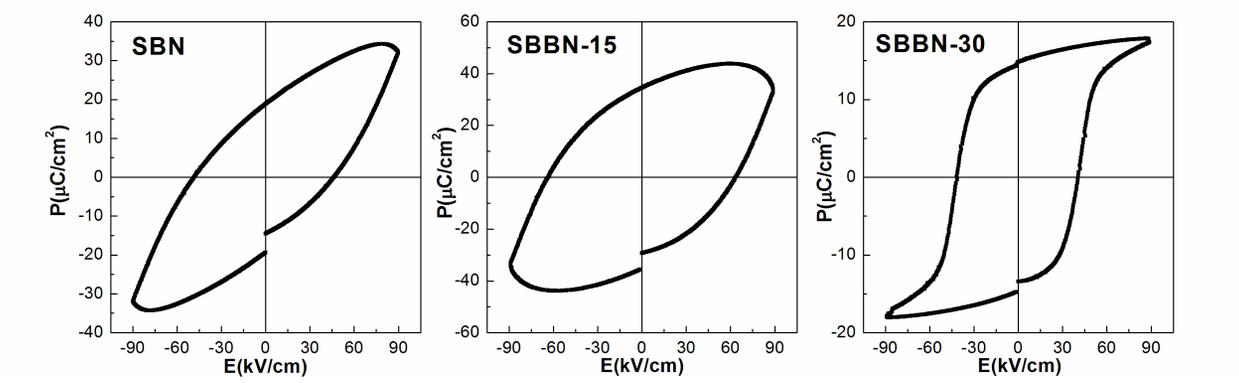

Figure 4. Polarization (*P*) dependence on the applied electric field (*E*), at room temperature, for samples with x ≤ 30 at %.

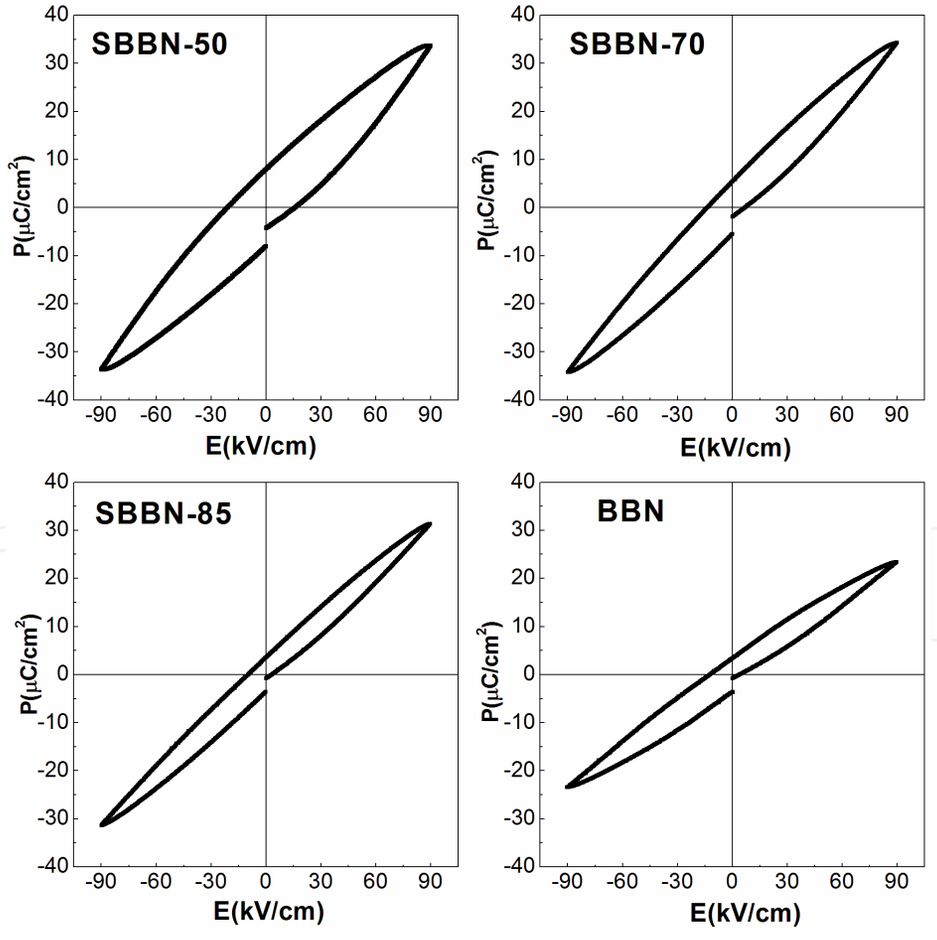

Figure 5. Polarization (*P*) dependence with the applied electric field (*E*), at room temperature, for samples with x ≥ 50 at%.

Composition	P_r ($\mu C/cm^2$)	P_r/P_{max}	E_c (kV/cm)
SBN	18.96	0.55	45
SBBN-15	34.48	0.80	63
SBBN-30	13.45	0.75	42
SBBN-50	8.10	0.24	22
SBBN-70	5.44	0.16	14
SBBN-85	3.68	0.11	12
BBN	3.55	0.14	13

Table 1. Values of the remanent polarization (P_r), P_r/P_{max} relationship and the coercive field (E_c) for the studied samples at room temperature.

Table 1 shows the values of the remanent polarization (P_r), the P_r/P_{max} relationship and the coercive electric field (E_c), at room temperature, for the studied compositions. P_{max} is the polarization at the highest applied electric field. The SBN and SBBN-15 samples show the highest P_r values. This is associated with higher dielectric losses for theses samples. The compositions with x ≥ 50 at% show the lower P_r values. These ceramics have also presented lower piezoelectric activity [37]. The sample with 30 at% of barium shows the better ferroelectric response with a high P_r value and a P_r/P_{max} relation, showing a good saturation. For this composition, a better piezoelectric response has been reported [37]. The E_c values tend to decrease with the increase of barium concentration. For compositions with x ≤ 50 at%, the E_c values are higher than those for other ferroelectrics materials from the Aurivillius family [35].

3.2. Thermally stimulated processes and pyroelectricity

Figure 6 and Figure 7 show the dependence of the thermally stimulated current (i) on the temperature in the studied samples. The black points represent the experimental curve and the lines represent the fitting, which was carried out using the Gaussian method.

For the compositions with x ≤ 30 at% (Figure 6), three different contributions were observed below the transition temperature (T_m). The contribution at higher temperatures (blue line) is observed from the increase of i at temperatures near to and higher than the transition temperature. The pyroelectric contribution is characterized by an increase to a maximum value, when the temperature (T) increases, and then a decrease to zero at the ferroelectric-paraelectric phase transition temperature. From this point of view, the third contribution is not the pyroelectric contribution.

The dielectric analysis of the studied samples has shown a strong influence of the electric conductivity on the dielectric parameters at the higher temperature range [22]. The third contribution could be associated with the electric conductivity processes in this temperature range. The influence of this contribution on the second (black line) is remarkable; this second contribution must be associated with the pyroelectric response. The first contribution (red line)

http://dx.doi.org/10.5772/60433

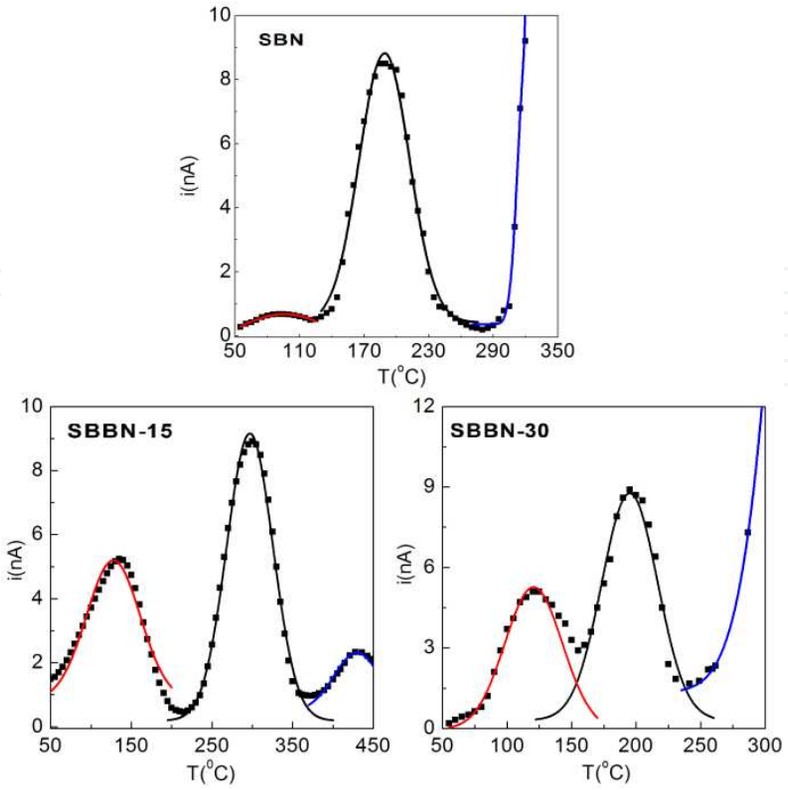

Figure 6. Thermally stimulated current curves (i) in a wide temperature range for the SBN, SBBN-15 and SBBN-30 samples. The black points show the experimental data and the red line (first contribution), black line (second contribution) and blue line (third contribution) represent the fitting using the Gaussian method.

is observed at the lower temperature range; it could not be associated with the pyroelectric response or electrical conductivity processes.

The compositions with x > 30 at% show the three contributions for temperatures lower than T_m as well (Figure 7).

From the theoretical curves $i(T)$, which were obtained by using the Gaussian method, the values of the relaxation time (τ) were calculated (equation 1). The temperature dependence for τ (Figures 8 and 9) was obtained for the first and second contributions, showing a typical Arrhenius dependence (equation 2). The values of ln τ are represented by points and the lines represent the fitting using equation 2. From the fitting, the corresponding activation energy values (U) for each contribution were obtained, and are shown in Table 2.

The activation energy values for the first contribution are between 0.40 and 0.60 eV. This contribution is observed in the lower temperature range, showing lower current values than those obtained for the second contribution. The first contribution could be related to space charge, which is injected during the polarization process. For the second contribution, which is associated with the pyroelectric current, the activation energy values tend to increase with the increase of the barium concentration until 30 at%; above that concentration, this parameter decreases.

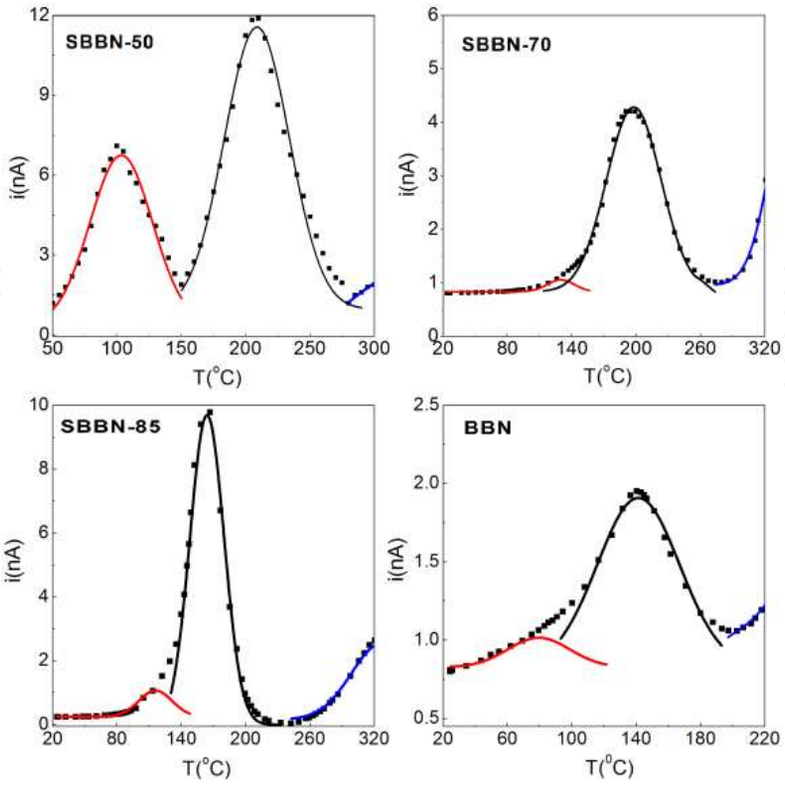

Figure 7. Thermally stimulated current curves (*i*) in a wide temperature range for the compositions with x > 30 at%. The black points show the experimental data and the red line (first contribution), black line (second contribution) and blue line (third contribution) represent the fitting using the Gaussian method.

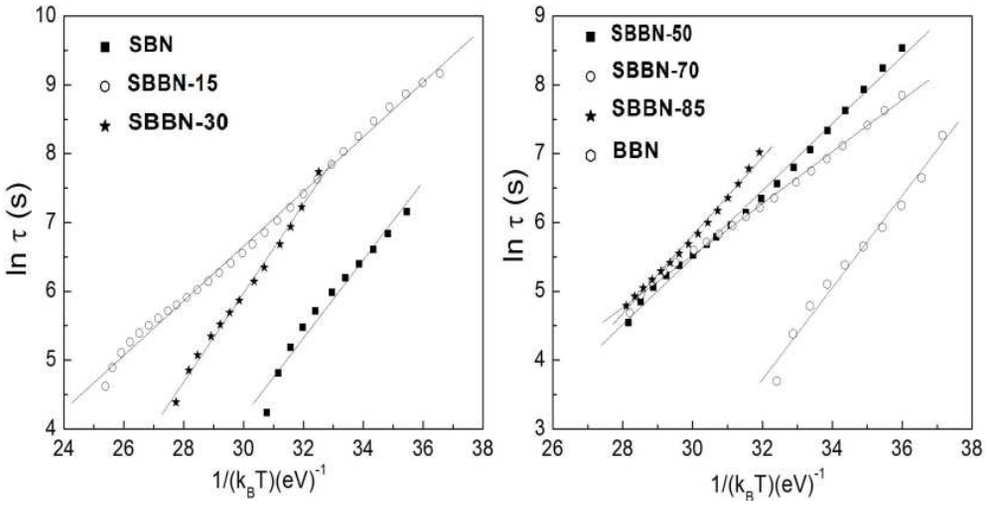

Figure 8. Arrhenius dependence of the first contribution on the *i-T* dependence. The solid points correspond to the relaxation time values, which were obtained using equation 1; the solid lines correspond to the fitting using equation 2.

For materials from the Aurivillius family, the major contribution to the spontaneous polarization comes from the motion of the *A* cation in the perovskite blocks [20, 23, 26]. The analysis of the dielectric behaviour for the studied samples has shown a lower ferroelectric-paraelectric

http://dx.doi.org/10.5772/60433

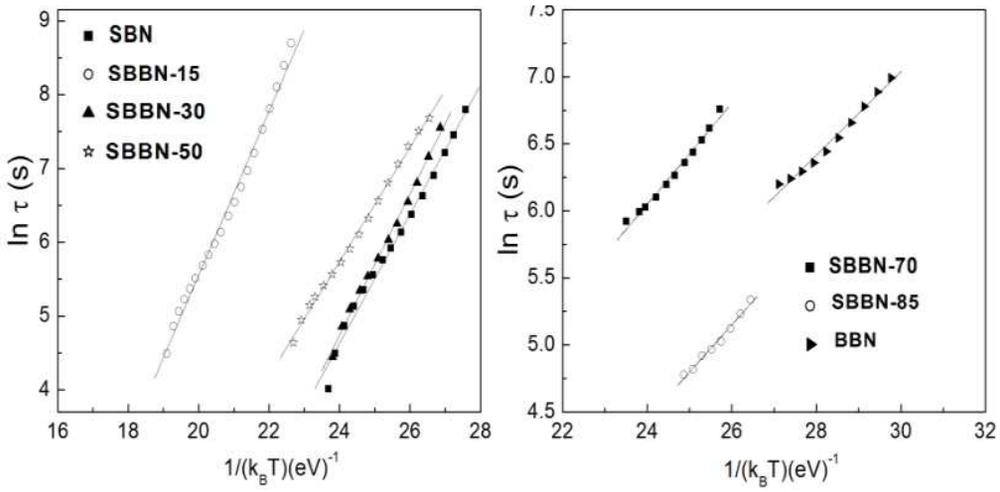

Figure 9. Arrhenius dependence of the second contribution on the *i-T* dependence. The solid points correspond to the relaxation time values, which were obtained using equation 1; the solid lines correspond to the fitting using equation 2.

transition temperature for the SBN sample [22] than that of the previous report [20]. This result suggests a decrease of the thermal energy, which is necessary to transition from a ferroelectric phase to a paraelectric phase. The structural study for this composition has also shown a higher occupancy of Bi^{3+} in *A* sites of the structure [22] than previous reports [14], which can explain the lower T_m value considering the lower radii ionic of the Bi^{3+} than that of the Sr^{2+}. Therefore, a lower activation energy value is necessary for the thermal depoling (pyroelectric contribution) of the studied SBN sample compared to previous reports. The SBBN-15 and SBBN-30 samples show an increase of the activation energy value with respect to the SBN composition, which is in agreement with the T_m behaviour from 0 to 30 at% [22].

Composition	First contribution U (eV)	Second contribution U (eV)
SBN	0.57	0.88
SBBN-15	0.40	1.11
SBBN-30	0.51	0.98
SBBN-50	0.49	0.82
SBBN-70	0.37	0.38
SBBN-85	0.57	0.35
BBN	0.60	0.33

Table 2. Activation energy values, which were obtained from the fitting shown in Figures 8 and 9.

For compositions with x > 30 at%, the activation energy values for the pyroelectric contribution have shown a decrease with the increase of the barium concentration in the structure. These results are in agreement with the dielectric behaviour of these compositions, which is shown

in a decrease of the T_m values when the barium concentration increases [22]. The SBBN-50 and SBBN-70 samples have shown a greater increase in the occupancy of Ba^{2+} and Bi^{3+} in *A* sites than was observed in the SBBN-30, since the concentration of Ba^{2+} is higher than that of Bi^{3+}, which explains the decrease of T_m from 30 to 70 at% of barium and then by extension the lower activation energy values for the pyroelectric contribution.

For SBBN-85 and BBN, a greater decrease of the Ba^{2+} occupancy in *A* sites is observed than in SBBN-70 [22], but the T_m values are lower. For both compositions, it has also been reported that there is a higher Ba^{2+} occupancy in Bi^{3+} sites than in the other compositions [22]. A higher Ba^{2+} occupancy in Bi^{3+} sites and the corresponding generated oxygen vacancies would distort the ionic dipoles due to the *A* sites' ions. Then, the decay of the spontaneous polarization could be affected, providing a decrease of the T_m values and the activation energy values for the thermal depoling process (pyroelectric response).

For the third contribution, there were not enough experimental points in some compositions. Thus, the activation energy was only estimated for the studied samples, showing values between 0.7 and 1.50 eV. These values are related to electrical conductivity processes, which are governed by double ionized oxygen vacancies [21, 24]. The oxygen vacancies in the structure of the studied samples are generated to compensate the electrical charge unbalance, which is caused by the substitution of trivalent Bi^{3+} ion for divalent Ba^{2+} and Sr^{2+} ions.

3.3. Ferroelectric and pyroelectric parameters

Figure 10 shows the temperature dependence of the remanent polarization (P_r), which has been obtained from the pyroelectric current dependence $i_P(T)$ using equation 3. It can be noted that there is an important influence of the barium concentration on the P_r values. At room temperature, an increase of P_r is observed for the lower barium concentration (x ≤ 30 at%); above 30 at%, P_r decreases. These results are in agreement with the P_r behaviour, which has previously been discussed in relation to the hysteresis loops (*P-E* dependence).

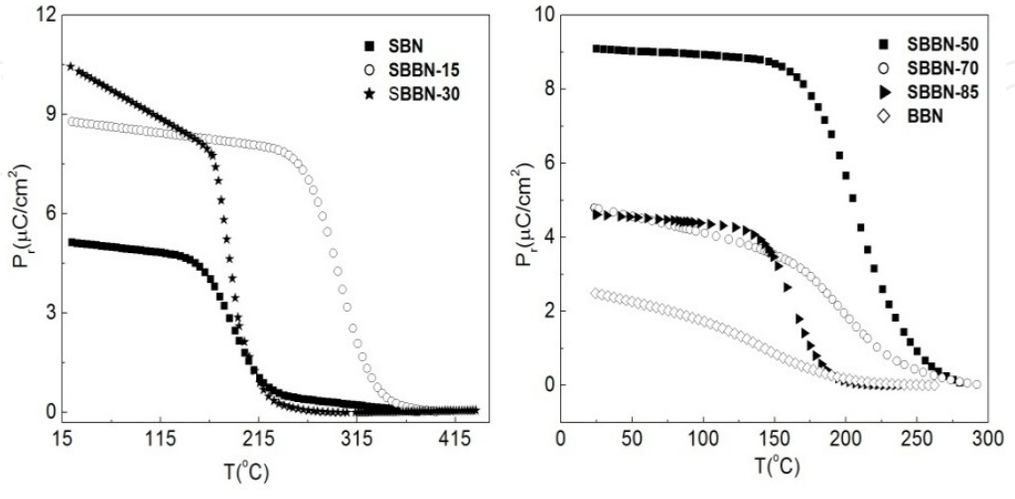

Figure 10. Temperature dependence of the remanent polarization (P_r) for the studied compositions.

http://dx.doi.org/10.5772/60433

Composition	P_r ($\mu C/cm^2$)	p ($\mu C/m^2$ °C)	R_V ($\mu C/m^2$ °C)
SBN	5.03	34	0.12
SBBN-15	8.63	38	0.16
SBBN-30	10.4	73	0.62
SBBN-50	9.02	20	0.07
SBBN-70	4.79	4	0.01
SBBN-85	4.61	10	0.04
BBN	2.49	4	0.02

Table 3. Values of the remanent polarization (P_r), the pyroelectric coefficient (p) and the current response parameter (R_V).

Table 3 shows the values for the remanent polarization (P_r), the pyroelectric coefficient (p) and the current response parameter (R_V), at room temperature, for the studied samples. The last two parameters were obtained using equations 4 and 5, respectively. The SBBN-30 sample shows the better pyroelectric parameter. The values for the pyroelectric parameters are analogous to previous reports in other Aurivillius materials [24]. However, these are lower than those for conventional lead-based ferroelectric systems [38-39]. Further researches are in progress.

4. Conclusions

The ferroelectric properties and thermally stimulated processes were studied in the $Sr_{1-x}Ba_xBi_2Nb_2O_9$ ferroelectric ceramic system with x = 0, 15, 30, 50, 70, 85, 100 at%. The dependence of the polarization on the applied electric field was discussed, at room temperature, for normal and relaxor ferroelectric compositions. The Gaussian method was used to separate the pyroelectric contribution from the other contributions to the total i(T) response in the studied samples. Three different contributions were obtained in the studied temperature range. The first contribution was associated with space charge, the second with the pyroelectric current and the third with the electric conductivity processes. The remanent polarization, the pyroelectric coefficient and the current response merit figure were evaluated at room temperature. The SBBN-30 showed better ferroelectric and pyroelectric properties.

Acknowledgements

The authors would like to acknowledge the Third World Academy of Sciences (RG/PHYS/LA Nos. 99-050, 02-225 and 05-043), and the ICTP, Trieste-Italy, for financial support of the Latin-American Network of Ferroelectric Materials (NET-43). Thanks to CNPq and FAPEMIG agencies of Brazil. Dr Aimé Peláiz-Barranco acknowledges Le Conseil Régional de Languedoc-

Roussillon for her invitation to the University of Nîmes, France. Thanks to the Embassy of France in Havana, Cuba, for financial support for the scientific cooperation between the University of Nîmes and Havana University. Dr Aimé Peláiz-Barranco would like to thank Tongji University, Shanghai, China.

Author details

Aimé Peláiz-Barranco[1*], Yuslín González Abreu[1], José de los Santos Guerra[2], Jinfei Wang[3,4], Tongqing Yang[3] and Pierre Saint-Grégoire[5]

*Address all correspondence to: pelaiz@fisica.uh.cu

1 Facultad de Física - Instituto de Ciencia y Tecnología de Materiales, Universidad de La Habana. San Lázaro y L, Vedado. La Habana, Cuba

2 Grupo de Ferroelétricos e Materiais Multifuncionais, Instituto de Física, Universidade Federal de Uberlândia. Uberlândia – M G, Brazil

3 Functional Materials Research Laboratory, College for Materials Science and Engineering, Tongji University, Caoan, Shanghai, China

4 Dwo Chemical (China) Investment, LTD. Pudong district, Shanghai, China

5 University of Nîmes, Department of Sciences and Arts, Nimes cedex, France

References

[1] Xu Y. Ferroelectric Materials and Their Applications. The Netherlands: Elsevier Science Publishers B.V.; 1991.

[2] Haertling GH. Ferroelectric ceramics: History and technology. Journal of the American Ceramic Society 1999; 82(4) 797-818.

[3] Ivan IA, Rakotondrabe M, Agnus J, Bourquin R, Chaillet N, Lutz P, Poncot J, Duffait R, Bauer O. Comparative material study between PZT ceramic and newer crystalline PMN-PT and PZN-PT materials for composite bimorph actuators. Advanced Materials Science 2010; 24(15-16) 1-9.

[4] Rauls MB, Dong W, Huber JE, Lynch CH. The effect of temperature on the large field electromechanical response of relaxor ferroelectric 8/65/35 PLZT. Acta Materialia 2011; 59(7) 2713-2722.

[5] Li F, Zhang S, Xu Z, Wei X, Luo J, Shrout TR. Temperature independent shear piezoelectric response in relaxor-$PbTiO_3$ based crystals. Applied Physics Letters 2010; 97(25) 252903.

[6] Li F, Zhang S, Lin D, Luo J, Xu Z, Wei X, Shrout TR. Electromechanical properties of $PbIn_{1/2}Nb_{1/2}O_3$–$PbMg_{1/3}Nb_{2/3}O_3$–$PbTiO_3$ single crystals. Journal of Applied Physics 2011; 109(1) 014108.

[7] Wang H, Ren MF. Characteristics of Ag/$Bi_{3.25}La_{0.75}Ti_3O_{12}$/p-Si heterostructure prepared by sol-gel processing. Journal of Sol-Gel Science and Technology 2007; 42(3) 247-250.

[8] Zhang H, Yan H, Reece MJ. Microstructure and electrical properties of Aurivillius phase $(CaBi_2Nb_2O_9)_{1-x}(BaBi_2Nb_2O_9)_x$ solid solution. Journal of Applied Physics 2010; 108(1) 014109.

[9] Yi ZG, Li YX, Liu Y. Ferroelectric and piezoelectric properties of Aurivillius phase intergrowth ferroelectrics and the underlying materials design. Physica Status Solidi A 2011; 208(5) 1035-1040.

[10] Cui Y, Fu X, Yan K. Effects of Mn-doping on the properties of $BaBi_4Ti_4O_{15}$ bismuth layer structured ceramics. Journal of Inorganic and Organometallic Polymers and Materials 2012; 22(1) 82-85.

[11] Aurivillius B. Mixed bismuth oxides with layered lattice. I. Ark. Kemi 1949; 1(54) 463-480.

[12] Wachsmuth B, Zschech E, Thomas N, Brodie S, Gurman S, Baker S, Bayliss S. Structure model of Aurivillius compounds. Physica Status Solidi A 1993; 135(1) 59-71.

[13] Ismunandar, KB. Structure of $ABi_2Nb_2O_9$ (A = Sr, Ba): Refinement of powder neutron diffraction data. Journal of Solid State Chemistry 1996; 126 136-141.

[14] Blake S, Falconer M, McCreedy M, Lightfoot P. Cation disorder in ferroelectric Aurivillius phases of the type $Bi_2ANb_2O_9$ (A=Ba, Sr, Ca). Journal of Materials Chemistry 1997; 7(8) 1609-1613.

[15] Mercurio D, Trolliarda G, Hansenb T, Mercurio J. Crystal structure of the ferroelectric mixed Aurivillius phase $Bi_7Ti_4NbO_{21}$. International Journal of Inorganic Materials 2000; 2(5) 397-406.

[16] Perez-Mato J, Aroyo M, García A, Blaha P, Schwarz K, Schweifer J, Parlinski K. Competing structural instabilities in the ferroelectric Aurivillius compound $SrBi_2Ta_2O_9$. Physics Review B 2004; 70(21) 214111.

[17] Haluska M, Misture S. Crystal structure refinements of the three-layer Aurivillius ceramics $Bi_2Sr_{2-x}A_xNb_2TiO_{12}$(A=Ca, Ba; x= 0, 0.5, 1) using combined x-ray and neutron powder diffraction. Journal of Solid State Chemistry 2004; 177(6) 1965-1975.

[18] Newnham R, Wolfe R, Dorrian J. Structural basis of ferroelectricity in the bismuth titanate family. Materials Research Bulletin 1971; 6 1029-1040.

[19] Newnham R, Wolfe R, Horsey R, Diaz-Colon F. Crystal structure of (Sr,Ba)$Bi_2Ta_2O_9$. Materials Research Bulletin 1973; 8(10) 1183-1195.

[20] Huang S, Feng Ch, Chen L, Wang Q. Relaxor behavior of $Sr_{1-x}Ba_xBi_2Nb_2O_9$ ceramics. Journal of the American Ceramic Society 2006; 89(1) 328-331.

[21] Wu Y, Forbess MJ, Seraji S, Limmer SJ, Chou TP, Nguyen C, Cao GZ. Doping effect in layer structured $SrBi_2Nb_2O_9$ ferroelectric. Journal of Applied Physics 2001; 90 5296-6002.

[22] González-Abreu Y, Peláiz-Barranco A, Guerra JDS, Gagou Y, Saint-Grégoire P. From normal ferroelectric transition to relaxor behavior in Aurivillius ferroelectric ceramic. Journal of Materials Science 2014; 49(21) 7437-7444.

[23] Peláiz-Barranco A, González-Abreu Y. Dielectric relaxation mechanisms in relaxor bi-layered perovskites. Ferroelectrics 2012; 426(1) 122-131.

[24] Peláiz-Barranco A, González-Abreu Y. Ferroelectric ceramic materials of the Aurivillius family. Journal of Advanced Dielectrics 2013; 3(4) 1330003.

[25] Ismunandar, Kennedy BJ. Effect of temperature on cation disorder in $ABi_2Nb_2O_9$ (A=Sr, Ba). Journal of Materials Chemistry 1999; 9(2) 541-544.

[26] González-Abreu Y, Peláiz-Barranco A, Aráujo EB, Franco Júnior A. Dielectric relaxation and relaxor behavior in bilayered perovskites. Applied Physics Letters 2009; 94(26) 262903.

[27] Cross LE. Relaxor ferroelectrics: An overview. Ferroelectrics 1994; 151(1) 305-320.

[28] Liu W, Randall CA. Thermally stimulated relaxation in Fe-doped $SrTiO_3$ systems: II. Degradation of $SrTiO_3$ dielectrics. Journal of the American Ceramic Society 2008; 91(10) 3251-3257.

[29] Almeida A, Correira TM, Chaves MR, Vilarinho PM, Kholkin AL, Costa AM. Study of polar relaxation processes in $Sr_{(1-1.5x)}La_xTiO_3$ ceramics by using field-induced thermally stimulated currents. Journal of the European Ceramic Society 2008; 27(13) 3701-3703.

[30] Peláiz Barranco A, Calderón Piñar F, Pérez Martínez O. Pyroelectricity and mechanisms of conductivity in $PbZr_{0.53}Ti_{0.47}O_3$ + 2.5 mol% La_2O_3 ferroelectric ceramics. Journal of Material Science Letters 2001; 20(15) 1439-1441.

[31] Chen R, Krish Y. Analysis of Thermally Stimulated Processes. Oxford: Pergamon Press; 1981.

[32] Faubert F, Sánchez M. Numerical decomposition of a complex thermostimulated depolarization current spectrum in single time relaxation peaks. Journal of Applied Physics 1998; 84(3) 1541-1545.

[33] Chen R, Haber G. Calculation of glow curves activation energies by numerical initial rise method. Chemistry Physics Letters 1968; 2(7) 483-485.

[34] Grossweiner LI. A note on the analysis of first-order glow curves. Journal of Applied Physics 1953; 24(10) 1306-1307.

[35] Kong LB, Ma J, Zhu W, Tan OK. Preparation of $Bi_4Ti_3O_{12}$ ceramics via a high-energy ball milling process. Material Letters 2001; 51(2) 108-114.

[36] Hou J, Vaish R, Ou Y, Krsmanovic D, Varma KBR, Kumar RV. Dielectric, pyroelectric and ferroelectric properties of $Bi_4Ti_{2.98}Nb_{0.01}Ta_{0.01}O_{12}$ Ceramics. Materials Chemistry Physics 2010; 121(1-2) 32-36.

[37] González-Abreu Y, Peláiz-Barranco A, Guerra JDS, Saint-Grégoire P. Piezoelectric behavior in $Sr_{1-x}Ba_xBi_2Nb_2O_9$ Aurivillius-type structure ferroelectric ceramics. Physica Status Solidi B 2013; 250(8) 1-5.

[38] Zhang MF, Wang Y, Wang KF, Zhu JS, Liu J-M. Characterization of oxygen vacancies and their migration in Ba-doped $P(Zr_{0.52}Ti_{0.48})O_3$ ferroelectrics. Journal of Applied Physics 2009; 105(6) 061639.

[39] Peláiz-Barranco A, García-Wong AC, González-Abreu Y, Gagou T, Saint-Grégoire P. Thermally stimulated processes in samarium-modified lead titanate ferroelectric ceramics. Applied Physics A 2013; 112(2) 419-423.

IntechOpen